Biomass Burning Influences on the Composition of the Remote South Pacific Troposphere: Analysis Based on Observations from PEM-Tropics-A

H. B. Singh[1], W. Viezee[1], Y. Chen[1], J. Bradshaw[2], S. Sandholm[2], D. Blake[3], N. Blake[3], B. Heikes[4], J. Snow[4], R. Talbot[5], G. Gregory[6], G. Sachse[6], S. Vay[6]

1. NASA Ames Research Center, Moffett Field, CA 94035
2. Georgia Institute of Technology, Atlanta, GA 30332
3. University of California, Irvine, CA 92717
4. University of Rhode Island, Narragansett, RI 02882
5. University of New Hampshire, Durham, NH 03824
6. NASA Langley Research Center, Hampton, VA 23665

(submitted to Atmospheric Environment, April 1999)

ABSTRACT

Airborne, in-situ measurements from PEM-Tropics-A (September/October 1996) are analyzed to show the presence of distinct pollution plumes in the middle-tropical troposphere of the remote South Pacific (10-30'S). These elevated plumes cause a relative maximum at about 5-7 km altitude in the vertical distribution of primary and secondary species characteristic of fuel combustion and biomass burning (CO, C_2H_2, C_2H_6, CH_3Cl, PAN, O_3). Similar plumes were also observed at mid-latitudes in the middle troposphere during three flights east of New Zealand (40-45'S). In all, pollution plumes with CO larger than 100 ppb were observed 24 times on 7 separate flight days south of the equator. The observed plumes were generally embedded in very dry air. Ten-day back trajectory analysis supports the view that these originated from the biomass burning regions of South Africa (and South America) and were transported to the South Pacific along long-distance subsiding trajectories. The chemical composition of the southern Pacific troposphere analyzed from the PEM-Tropics-A data is compared with data from the tropical regions of the northern Pacific (PEM-West-A) and southern Atlantic (TRACE-A) during the same Sept/Oct time period. Sizable perturbations in the abundance of ozone and its key precursors, resulting from the transport of pollution originating from biomass burning sources, are observed in much of the Southern Hemispheric troposphere.

INTRODUCTION

The NASA Global Tropospheric Experiment (GTE) aims to elucidate the composition and chemistry of the earth's atmosphere through a series of airborne field experiments (McNeal et al., 1983). The tropical marine regions of the atmosphere are thought to be relatively free of direct influences from man-made pollution. Significant industrial growth in Asia and biomass burning pollution in Africa and South America have the potential to greatly impact these pristine tropical regions. The environmental consequences of such pollution are diverse and include emission of acidic gases leading to acidic precipitation, release of particles that can impact cloud formation and precipitation, and release of photochemical precursors (hydrocarbons and NO_X) that can result in widespread production of ozone in the troposphere (Crutzen and Andreae, 1990; Fishman et al., 1991; Lacaux et al., 1992; Jacob et al., 1996; Davis et al., 1996). As part of GTE, a field experiment [Pacific Exploratory Mission (PEM)-Tropics-A] was performed in September/October 1996 to explore the south central Pacific region in search of nearly unpolluted air. PEM-Tropics-A complemented two previous GTE missions conducted during the same months in the western Pacific (PEM-West-A; 1991) and South Atlantic (TRACE-A: Transport and Atmospheric Chemistry near the Equator-Atlantic; 1992). While PEM-West-A explored the industrial outflow from Asian countries, TRACE-A largely concentrated on sampling biomass burning pollution from Africa and South America. In all cases an instrumented NASA DC-8 aircraft was utilized for airborne measurements to 12-km altitudes.

The geographical coverage of the PEM-Tropics-A missions is shown in Figure 1. The NASA DC-8 flew 14 missions in the South Pacific covering areas from the equator to about 45°S and from 155°E to 110°W. An exploratory flight to the Arctic was also conducted. Distributions of important trace chemicals observed in the troposphere are analyzed with a focus on the potential impact of biomass burning pollution. Measurements obtained during PEM-West-A, TRACE-A, and PEM-Tropics-A are compared. Experimental and meteorological details of PEM-West-A (Hoell et al., 1996), TRACE-A (Fishman et al., 1996) and PEM-Tropics-A (Hoell et al., 1998; Fuelberg et al., 1998) can be found in the available literature.

1. PEM-TROPICS-A COMPARISONS WITH PEM-WEST-A AND TRACE-A

Figure 2 shows latitudinal profiles of select species characteristic of primary and secondary products of continental and biomass combustion (CO, C_2H_2, NO_X, PAN, HNO_3 and O_3) in the free troposphere. NO_X is defined as the sum of the measured NO and NO_2. It has been shown that during PEM-Tropics-A there was good agreement between measured NO_2 and that derived from measured NO (Bradshaw et al., 1998). The profiles are obtained by averaging data from all PEM-Tropics-A missions shown in Figure 1 for the middle (4-8 km; 600-400 mb) and upper (8-12 km; 400-200 mb) troposphere over 10° latitude bins. As is evident from Figure

1, the density of data was the greatest between 0 and 30°S with more limited coverage elsewhere. The most salient feature of these latitudinal profiles (Figure 2) is the enhancement in the mixing ratio of key chemicals in the Southern Hemisphere. In virtually all cases (e. g. CO, C_2H_2, PAN, HNO_3) these enhancements are larger in the middle troposphere than in the upper troposphere. The SH mixing ratios of tracer species CO, C_2H_2, and PAN also showed high correlation (R^2=0.8-0.9) with wind speed for the middle troposphere that allude to the important role of transport as further discussed below.

In the case of NO_x the larger mixing ratios were encountered in the upper troposphere where twin peaks at 25°N and 16-25°S were observed (Figure 2). The NO_x peak near 25°N is similar to that observed during PEM-West-B (Feb/Mar, 1994) in the western Pacific at 20-30°N. (Singh et al., 1998). Brunner (1998), based on sampling from instruments aboard commercial aircraft, reports the presence of persistent high NO_x mixing ratios in the upper troposphere throughout the NH. No ready explanation can be given for the observed NO_x maximum in the SH upper troposphere. However, meteorological analysis supports the possibility that these air masses encountered lightning during transport to the sampling region (Fuelberg et al., 1998). The mixing ratios of HNO_3 during Mission 4 just south of Hawaii at about 12°N were anomalously high. The concurrent presence of extremely low NO (10-15 ppt) suggests that this may have involved an aged plume in which most of the NO_x had been oxidized to HNO_3. There was further evidence of a tropical cirrus-cloud system in the vicinity and an evaporating cloud could have left behind HNO_3.

We now compare the vertical profiles of chemical data averaged for the tropical South Pacific (PEM-Tropics-A; 0-30°S, 100°W-160°E), central/western north tropical Pacific (PEM-West-A; 0-20°N, 160°W-120°E), and tropical South Atlantic (TRACE-A; 0-30°S, 10°E-30°W). Prior to any comparisons, it is instructive to examine Figure 3 which shows profiles of the ratio of C_2H_2/CO for the three tropical ocean regions. This ratio is a measure of the relative processing (age) of the air masses sampled (Smyth ET al, 1996). It is evident from Figure 3, that both the free troposphere of TRACE-A and the boundary layer of PEM-West-A have high values of this ratio. This suggests relatively recent contact with fresh pollution sources. During TRACE-A biomass burning emissions were the most likely sources of pollution [Talbot et al., 1996; Chatfield et al. 1996; Singh et al., 1996; Thompson et al., 1996], while during PEM-West-A it was the outflow of pollution from the Asian continent [Dibb et al., 1996; Talbot et al., 1996]. The air sampled during PEM-Tropics-A on the whole is associated with generally low values of the C_2H_2/CO ratio, that suggest an air mass aged with respect to input from pollution sources. A very similar picture also emerges from a detailed analysis of back trajectories and 3-D model simulations [Fuelberg et al., 1998; Chatfield et al., 1998].

Shown in Figure 4 (a) and 4 (b) are the vertical distributions of some primary and secondary tracers of varying solubility and lifetimes for the selected tropical marine regions. CO, C_2H_2, C_3H_8, and the long-lived CH_4 are insoluble tracers that are released during combustion and have atmospheric lifetimes that may range from weeks to years [Blake et al., 1998; Mauzerall et al., 1998]. In contrast, organic acids (CH_3COOH and HCOOH) are more soluble primary pollutants while peroxides (H_2O_2 and CH_3OOH) are soluble secondary pollutants. H_2O_2 is highly soluble and along with CH_3OOH provides a good indication of the degree of wet chemical removal. While the profiles of tropospheric temperature and water vapor content (not shown) were similar for the three areas and characteristic of the tropical atmosphere, some significant differences in the chemical profiles are apparent. The most profound of these is the difference in the mixing ratios of tracers observed during PEM-Tropics-A and TRACE-A. Air masses sampled in the South Atlantic during TRACE-A were greatly influenced by the presence of nearby biomass burning activity in Africa and by transport of the resulting pollution to the sampling region within 3 to 5 days (Singh et al., 1996) . The PEM-West-A data collected over the central/western north tropical Pacific represent the higher concentrations of tracers typically found in the NH [Blake et al., 1998]. The continental Asian outflow (Talbot et al., 1996) caused the marine boundary layer of the tropical North Pacific to be the most polluted area of the troposphere for the primary insoluble tracer species (Figure 4 a).

Hydrogen peroxide (H_2O_2), methylhydroperoxide (CH_3OOH) are secondary products of photochemistry and their high concentrations in the tropics reflect the greater availability of sunlight and moisture in this region. Unlike the peroxides, the organic acids are directly released by biomass burning emissions and the TRACE-A region was greatly influenced (Figure 4 b). In the upper troposphere, relatively low and near-uniform mixing ratios of soluble species attest to the effectiveness of the wet removal processes. Meteorological analysis supports the possibility that these air masses encountered clouds and rain during transport to the sampling region (Fuelberg et al., 1998).

Figure 5 shows vertical profiles of the reactive nitrogen species (NO_x, PAN and HNO_3) and O_3. These species have complex source and removal processes [Singh et al., 1996; Jacob et al., 1996]. The impact of pollution sources on these chemicals is clearly different than in the case of the biomass tracers. A comparison of these data clearly shows that significant perturbations in the ozone and reactive nitrogen fields are possible in regions far away from pollution sources. Indeed one could conclude that ozone perturbations of a factor of two or three are possible in the SH from the influence of these pollution sources and these regions can be more polluted than the tropical NH regions sampled in PEM-West-A. Another typical feature of these distributions is that the lowest mixing ratios are found in the marine boundary layer. The origin of tropospheric ozone and NO_x over the tropical south Pacific has been further analyzed by Schultz et al [1998] with the help of a photochemical model. They emphasize the important source of O_3 and NO_x from westerly transport into the region associated with biomass burning in Africa and South America.

2. POLLUTION PLUMES AND THEIR ORIGIN DURING PEM-TROPICS-A

Specific PEM-Tropics-A missions observed very distinct pollution plumes in the middle and upper troposphere. Pollution plumes defined as CO>100 ppb were observed 24 times on 7 separate missions south of the equator. During M12, a long flight from Tahiti to New Zealand, plumes were observed for a total cumulative time period of 1.5 hours. Large plumes were observed also on M13 east and just south of New Zealand. On other flights, narrow distinct plumes were detected for periods of up to 20 minutes. Most frequently, these plumes were present in the mid-troposphere (4-8 km), however, upper tropospheric pollution was also seen.

Figure 6a (top) shows an example of a CO pollution plume (maximum CO=113 ppb) observed during M6 when the DC-8 flew southward along 155°W longitude at 10 km altitude (see Figure 1). The plume, encountered when the plane emerged from cirrus clouds, was embedded in very dry air (80 ppm water vapor). At the same time as the dramatic CO increase and water vapor decrease, O_3 increased from 30 to 90 ppb while NO, PAN, and the NMHCs (not shown) increased similarly. The wind speed (not shown) increased to a maximum of 105 knots while the ambient temperature which had been steady at -42^{o} to -43 ^{o}C began a slight decrease. The observed gradients in both wind speed and temperature identified a minor airmass boundary. Trajectories relevant to the data of M6 published by Fuelberg et al., (1998) suggest that the cirrus clouds (equatorward of 25^{o}S) originated from possible thunderstorms in the equatorial areas near and north of the Fiji Islands while the dry pollution plumes that started at 25^{o}S arrived along subsiding westerly trajectories from across Australia and the Indian Ocean.

Figure 6b (bottom) also shows a CO plume centered at 6.5 km altitude observed during a descent near 30°S, 155°W from 10 km down to the marine boundary layer. The maximum CO concentration of 77 ppb was encountered when coming out of cirrus clouds at about 7 km altitude and coincided with dry air (100-200 ppm water vapor). In this case, two O_3 peaks were apparent, one near 5km the other at 7km. The nadir-looking DC-8 DIAL identified the location and magnitude of these two O_3 peaks precisely (Fenn et al., 1998). This CO plume has been further analyzed by Chatfield et al. (1998) using a 3-D model. Their computer simulations suggest that it was associated with the Southern Global Plume of CO and with long-range trajectories that tend to go back over or near the southern coast of Africa and as far as the southern tip of Brazil. The marine boundary layer shown in Figure 6b is characterized by low mixing ratios of ≈30 ppb O_3 and ≈50 ppb CO. In general., the marine boundary layer was only minimally influenced by pollution intrusions because of the presence of a strong temperature inversion.

Figure 7 shows vertical profiles of the mean mixing ratio of several principal species using the average of all data from M6 and data from M12 and M14 between 15°S and 30°S. These flights were clearly influenced by the presence of pollution plumes. A relative maximum in the mixing ratios of many species at 4-8 km altitude is evident. Methyl Chloride, a tracer of biomass burning pollution, is elevated along with other less specific tracers such as CO. Sharp maxima were also present for secondary photochemical species such as PAN, O_3 and HNO_3. Chemicals such as C_2Cl_4 (characteristic of urban pollution) were at their expected background levels.

Another property of the observed plumes was that they were most frequently embedded in very dry air. From a total of 100 CO measurements (1-min average) larger than 100 ppb collected in the area from the equator to 30°S, 73% were associated with dry air containing less than 1000 ppm water vapor. Out of these 73 observations, 46 observations (63%) were associated with very dry air of less than 200 ppm water vapor. These data are in accordance with the subsiding nature of the long-range trajectories of the pollution plumes. These large, extremely dry plumes should have unique photochemical and radiative properties that deserve further study.

In a recent study, Mauzerall et al (1998) examined the chemical characteristics of biomass burning plumes observed during TRACE-A. They calculated an enhancement ratio (ER), $\Delta Y/\Delta X$ where Y is a tracer of interest and X is a reference tracer such as CO or CO_2, as a function of time to determine plume age (fresh, recent, aged, and old). For example, their mean ER for the regression of C_2H_2 versus CO based on the analysis of a large number of plumes is 2.8 (ppt/ppb) for old plumes and 4.2 for a fresh plume. The decrease of ER with time is the result of the greater dilution with time for the selected tracer of interest than for the long-lived reference tracer CO. We calculated similar ER for a number of selected chemicals measured in PEM-Tropics-A. Figure 8 shows an example of the linear relationship found between C_2H_2 and PAN with that of CO using tracer data from M6, 12, and 14 between the 15°S and 30°S. Table 1 summarizes the ER calculated from such correlations and also presents the values determined by Mauzerall et al (1998) for characteristic old biomass-burning plumes for the TRACE-A region. The ER values for several species such as CH_4, C_2H_2, C_2H_6, CH_3Cl, PAN, O_3 are positive and comparable to those determined by Mauzerall. These further indicated that these plumes had the characteristics of emissions from biomass burning sources. There is no linear relationship seen between the abundance of peroxides (H_2O_2, CH_3OOH) and CO in the PEM-Tropics-A data. This is likely due to their high water solubility and selective removal via wet chemical processes during long range transport. The ER for NO_x (Table 1) is also quite different from that obtained by Mauzerall et al for old biomass-burning plumes. This is expected as NO_x in the PEM-Tropics-A study region was more controlled by sources such as lightning and recycling from PAN and HNO_3 than by long-range transport from its biomass burning locations (Schultz et al, 1998).

CONCLUSIONS

Chemical tracers of continental combustion and biomass burning collected during PEM-Tropics-A are analyzed to show that distinct pollution plumes were frequently present in the upper and middle troposphere of the remote tropical South Pacific. The observed pollution plumes originated from the biomass burning areas of South Africa and South America. It appears that biomass burning pollution is easily lofted into the free troposphere and transported throughout the Southern Hemisphere in the form of relatively broad plumes. While ozone and tracer levels in the free troposphere are strongly impacted, the marine boundary layer is only minimally influenced because of the strong temperature inversion. Many of the plumes were extremely dry and may have unique photochemical and radiative properties that should be studied further.

ACKNOWLEDGMENT: This research was supported by the NASA Global Tropospheric Experiment. We acknowledge all PEM-Tropics-A participants for their cooperation and support. Special thanks are due to the flight and ground crew of the NASA Ames Research Center for making this effort a success.

REFERENCES

Blake, N. J., D. R. Blake, O. Wingenter, B. Anderson, G. Gregory, G. Sachse, G. Kok and F. S. Rowland (1998) Influence of southern hemispheric biomass burning on the south Pacific mid-troposphere: Results from PEM-Tropics A and ACE-1, *J. Geophys. Res. 000*, in press.

Bradshaw, J. et al. (1998) Photofragmentation two-photon laser-induced fluorescence detection of NO_2 and NO: comparison of measurements with model results based on airborne observations during PEM-Tropics-A, *Geophys. Res. Lett. 00*, in press.

Brunner, D. W. (1998) One-Year Climatology of Nitrogen Oxides and Ozone in the Tropopause Region-Results from B-747 Aircraft Measurements, Diss. ETH No. 12556, submitted to the Swiss Federal Institute of Technology, Zurich, 1998.

Chatfield, R. B., Z. Guo, G. W. Sachse, N. Blake, D. Blake, and E. Browell (1998) Mechanism of the Southern Global Plume: How tropical burning plumes affect the remote Pacific, *J. Geophys. Res. 000*, submitted.

Chatfield, R. B., J. Vastano, H. Singh and G. Sachse (1996) A general model of fire emissions and chemistry African/oceanic plumes (O_3, CO, PAN, smoke) in TRACE A, *J. Geophys. Res. 101*, 24, 279-24,306.

Crutzen, P. J. and M. O. Andreae (1990) Biomass burning in the tropics: Impact on atmospheric chemistry and biogeochemical cycles, *Science*, *250*, 1669-1678.

Davis D. D. et al., 1996 An assessment of the photochemical ozone tendency in the western north Pacific, *J. Geophys. Res.*, *101*, 2111-2134.

Dibb J. et al. (1996) Asian influence over the western north Pacific during the fall season: inferences from Pb-210, soluble species and ozone", *J. Geophys. Res.*, *101*, 1779-1792.

Fenn et al. (1998) Ozone and aerosol distribution and air mass characteristics over the south Pacific during he burning season, *J. Geophys. Res. 000*, in press.

Fishman, J. et al. (1991) Identification of widespread pollution in the southern hemisphere deduced from satellite analysis, *Science 252*, 1693-1696, 1991.

Fishman, J. et al. (1996) The NASA GTE TRACE-A experiment (September-October, 1992): overview, *J. Geophys. Res.101*, 23,865-23,879.

Fuelberg, H. E. R. E. Newell, S. Longmore, Young Zhu, and D. J. Westberg, and E. V. Browell (1998) A Meteorological Overview of the PEM-Tropics Experiment, *J. Geophys. Res. 000*, in press.

Heikes, B., et al. (1996) Hydrogen peroxide and methylhydroperoxide distributions related to ozone and odd hydrogen over the north Pacific in the fall of 1991, *J. Geophys. Res. 101*, 1891-1905.

Hoell, J. M. Jr., et al. (1998) Pacific Exploratory Mission in the Tropics; September 1996, *J. Geophys. Res. 000*, in press.

Jacob, D. J. et al (1996) Origin of Ozone and NO_X in the tropical troposphere: A photochemical analysis of aircraft observations over the south Atlantic basin, *J. Geophys. Res. 101*, 24,235-24,250.

Lacaux, J. (1992) Precipitation chemistry in the Mayombe forest of equatorial Africa, *J. Geophys. Res.*, *97*, 6195-6206.

Logan, J. A., M. J. Prather, S. C. Wofsy, and M. B. McElroy (1981) Tropospheric chemistry: A global perspective, *J. Geophys. Res. 86*, 7210-7254.

Mauzerall, D. L., J. Logan, D. Jacob, B. Anderson, D. Blake, J. Bradshaw, B. Heikes, G. Sachse, H. Singh, and R. Talbot (1998) Photochemistry in biomass burning plumes and implications for tropospheric ozone over the tropical south Atlantic, *J. Geophys. Res. 103*, 8401-8423.

McNeal, R. J., J. P. Mugler, Jr., R. C. Harriss, and J. M. Hoell, Jr. (1983) NASA Global Tropospheric Experiment, *Eos Trans. AGU 64*, 561-562.

Schultz, M., D. J. Jacob, J. A. Logan, Y. Wang, D. Blake, J. Bradshaw, G. Gregory, G. Sachse, B. Heikes, R. Shetter, H. Singh, R. Talbot (1998) On the Origin of Tropospheric Ozone and NOx Over the Tropical South Pacific, *J. Geophys. Res. 000*, in press.

Smyth, S., S. Sandholm, S. Liu, S. McKeen, G. Gregory, B. Anderson, R. Talbot, D. Blake, S. Rowland, E. Browell, M. Fenn, J. Merrill, S. Bachmeier, G. Sachse, J. Collins, D. Thornton, D. Davis, and H. Singh (1996) Comparison of free tropospheric western Pacific air mass classification schemes for the PEM-West A experiment, *J. Geophys. Res. 101*, 1743-1762.

Singh, H. B. et al. (1996) Impact of biomass burning emissions on the composition of the south Atlantic troposphere, *J. Geophys. Res. 101*, 24,203-24,219.

Singh, H. B. et al. (1998) Latitudinal Distribution of Reactive Nitrogen in the Free Troposphere over the Pacific Ocean in Late Winter/Early Spring, *J. Geophys. Res. 103*, 28,237-28,246.

Talbot R. et al. (1996) Chemical characteristics of continental outflow from Asia to the western Pacific ocean during September-October 1991: results from PEM-West A, *J. Geophys. Res., 101*, 1713-1726.

Talbot, R. W., J. E. Dibb, E. M. Scheuer, J. D. Bradshaw, S. T. Sandholm, and H. B. Singh, D. Blake and N. Blake (1998) Distribution of tropospheric reactive odd nitrogen over the south Pacific Ocean in austral springtime, *J. Geophys. Res. 000*, in press.

Thompson, A. et al. (1996) Ozone over southern Africa during SAFARI-92/TRACE A, *J. Geophys. Res. 101*, 23,739-23,807.

FIGURES

Figure 1. Geographical coverage of the PEM-Tropics-A airborne expedition. This experiment took place from 30 August to 6 October 1996.

Figure 2. Average latitudinal distribution (10° bins) of selected reactive nitrogen species and primary tracers measured during PEM-Tropics-A

Figure 3. Vertical profiles for the tropical ocean areas PEM-Tropics-A, TRACE-A, and PEM-West-A of C_2H_2/CO identifying tropospheric layers of aged air (low values) and freshly polluted air (high values larger than 1.0).

Figure 4. Comparison between average vertical profiles of chemical tracers characteristic of continental combustion and biomass burning for the tropical ocean areas of PEM-Tropics-A (1996), PEM-West-A (1994), and TRACE-A (1992) (Sept/Oct period). For clarity the standard deviations for PEM-T-A are indicated only.

Figure 5. Comparison between average vertical profiles of selected reactive nitrogen species and ozone for the tropical ocean areas of PEM-Tropics-A, TRACE-A, and PEM-West-A (Sept/Oct period).

Figure 6. Pollution plumes observed during PEM-Tropics-A Mission 6 (Tahiti), 5 September 1966. (a) Horizontal flight at 10 km altitude (23°S – 29°S, 155°W); (b) Descent at 30°S, 155°W

Figure 7. Vertical profiles of tracers and reactive nitrogen species using the average of all data from PEM-Tropics-A Missions 6, 12, and 14 for the tropical troposphere between 15°S and 30°S.

Figure 8. Examples of linear correlation between selected tracers and the reference tracer CO using data from PEM-Tropics-A missions 6, 12, and 14 (10-30°S). Regression slopes identify enhancement ratios.

Table 1. Enhancement ratios (ER) derived from PEM-Tropics-A and TRACE-A measurements

Enhanced Ratios	PEM-Tropics-A ER (R^2)#	TRACE-A ER± SE*
$\Delta O_3/\Delta CO$ (ppb/ppb)	0.75 (0.56)	0.74±0.90
$\Delta CH_4/\Delta CO$ (ppb/ppb)	0.33 (0.39)	0.44±0.12
$\Delta CH_3Cl/\Delta CO$ (ppt/ppb)	0.59 (0.46)	1.43±0.13
$\Delta NO_x/\Delta CO$ (ppt/ppb)	0.47 (0.18)	3.3±1.4
$\Delta PAN/\Delta CO$ (ppt/ppb)	4.37 (0.81)	6.0±0.3
$\Delta H_2O_2/\Delta CO$ (ppt/ppb)	1.97 (0.01)	20.8±17.8
$\Delta CH_3OOH/\Delta CO$ (ppt/ppb)	-2.27 (0.02)	10.6±7.1
$\Delta C_2H_2/\Delta CO$ (ppt/ppb)	2.60 (0.92)	2.8±0.2
$\Delta C_2H_6/\Delta CO$ (ppt/ppb)	8.08 (0.88)	8.0±0.7

Data from missions 6, 12 and 14 (<30°S)

*Mean ER and Standard Error (SE) for Old plumes from Mauzerall, et al. (1998).

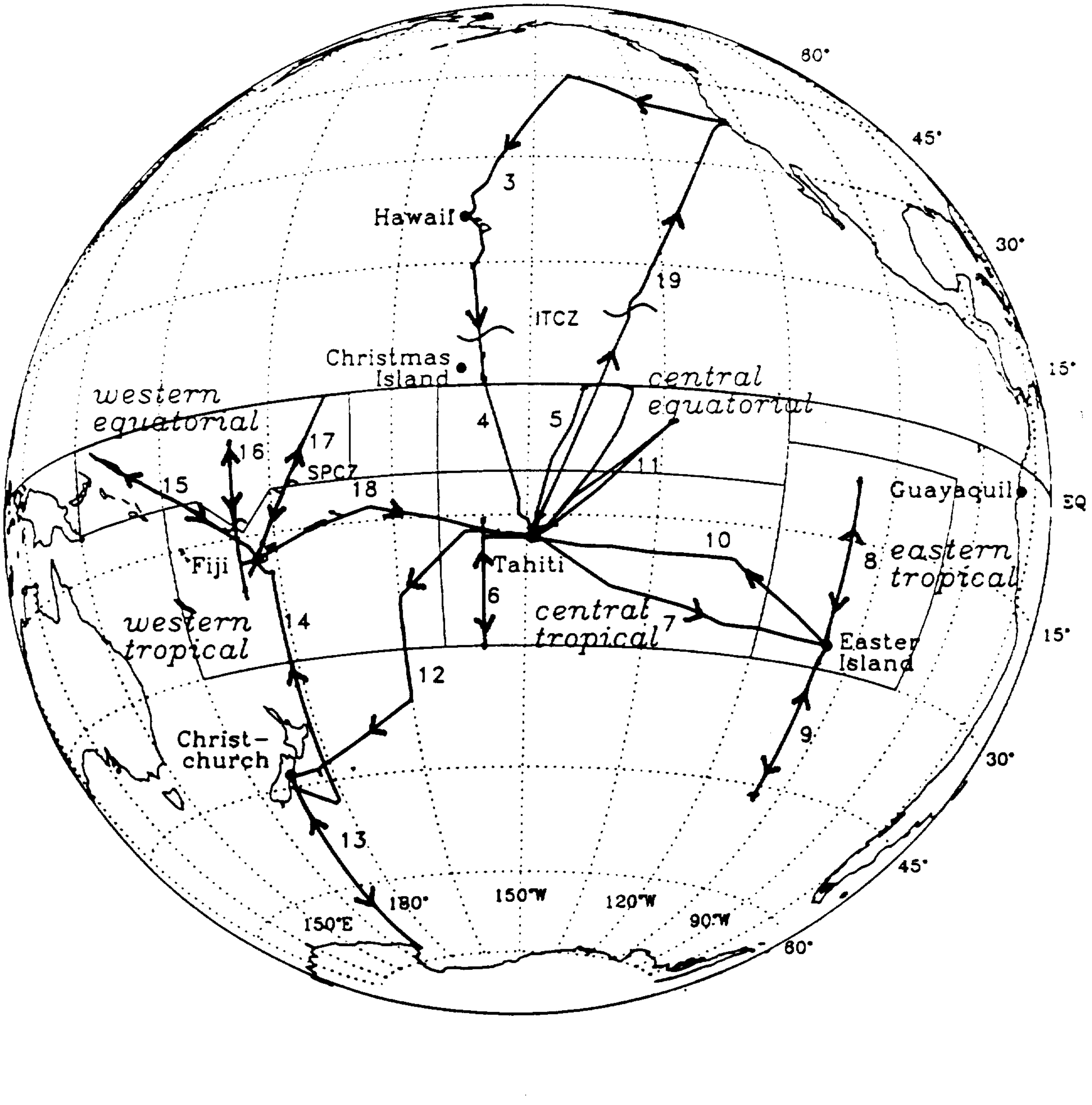

80°
45°
30°
15°
EQ
15°
30°
45°
80°
3
Hawaii
19
ITCZ
Christmas Island
central equatorial
western equatorial
4
5
11
16
17
SPCZ
15
18
Guayaquil
10
8
eastern tropical
Fiji
Tahiti
6
central tropical
7
western tropical
14
Easter Island
12
Christ-church
9
13
180°
150°W
120°W
90°W
150°E

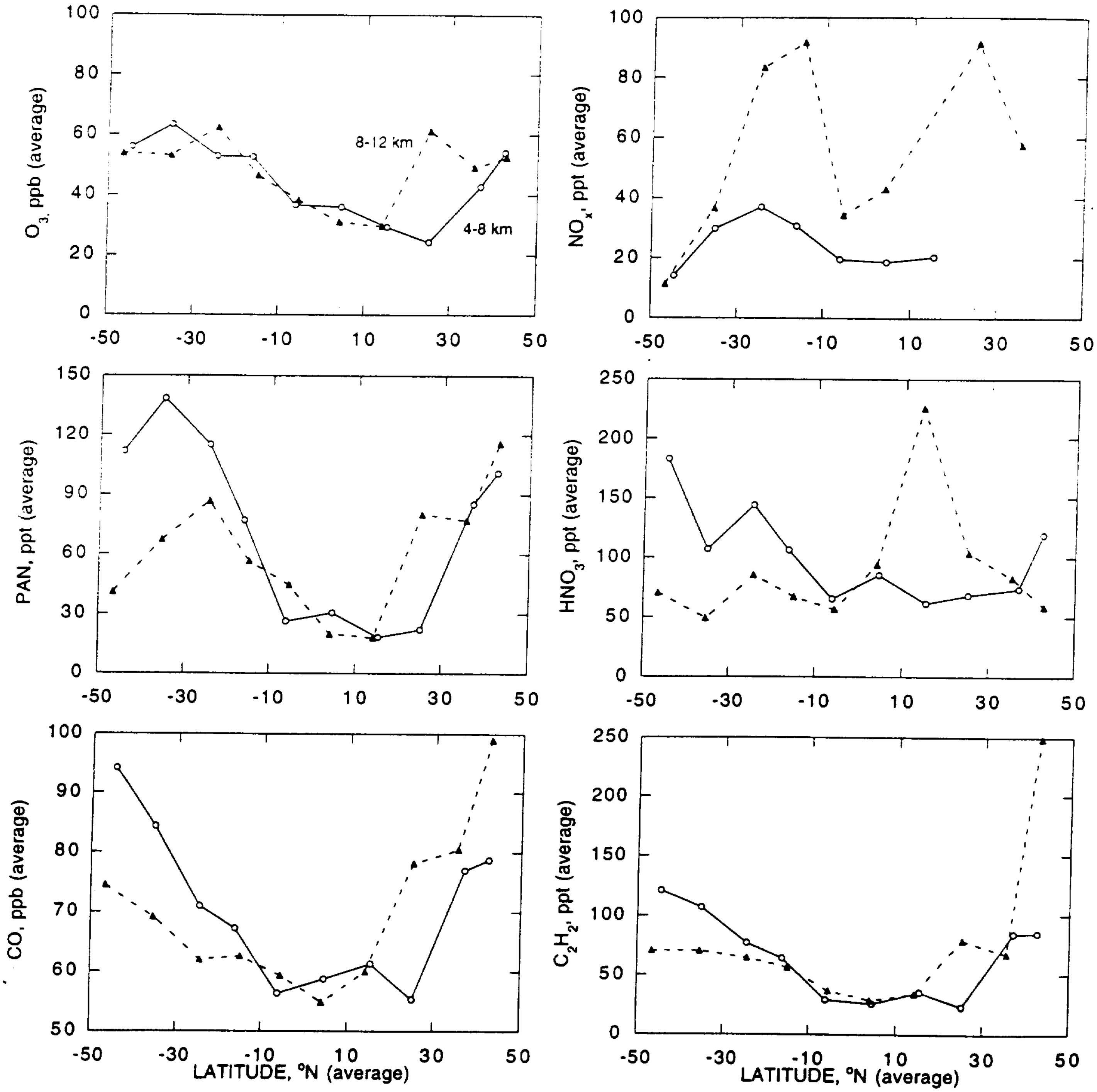
O$_3$, ppb (average)
8-12 km
4-8 km
NO$_x$, ppt (average)
PAN, ppt (average)
HNO$_3$, ppt (average)
CO, ppb (average)
C$_2$H$_2$, ppt (average)
LATITUDE, °N (average)
LATITUDE, °N (average)
-50
-30
-10
10
30
50
0
20
40
60
80
100
0
30
60
90
120
150
0
50
100
150
200
250
50
60
70
80
90
100

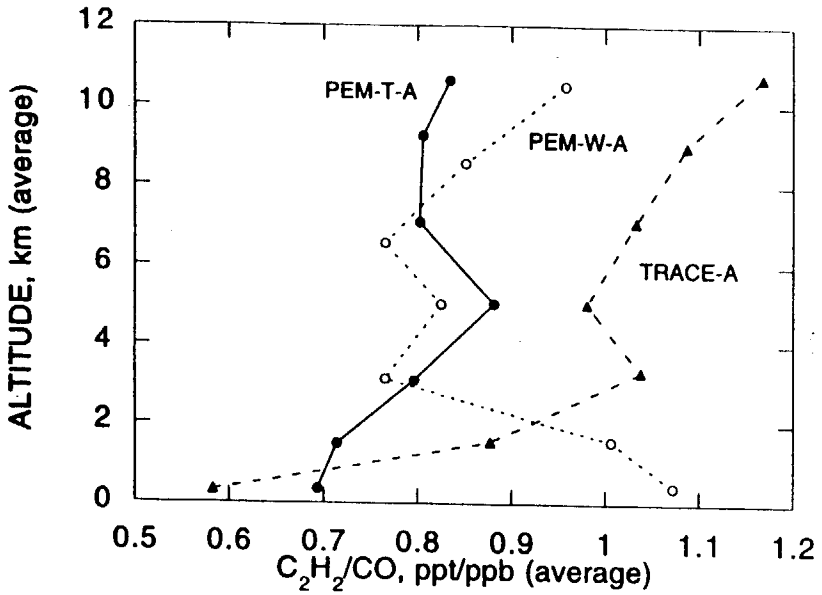
PEM-T-A
PEM-W-A
TRACE-A
ALTITUDE, km (average)
12
10
8
6
4
2
0
0.5
0.6
0.7
0.8
0.9
1
1.1
1.2
C_2H_2/CO, ppt/ppb (average)

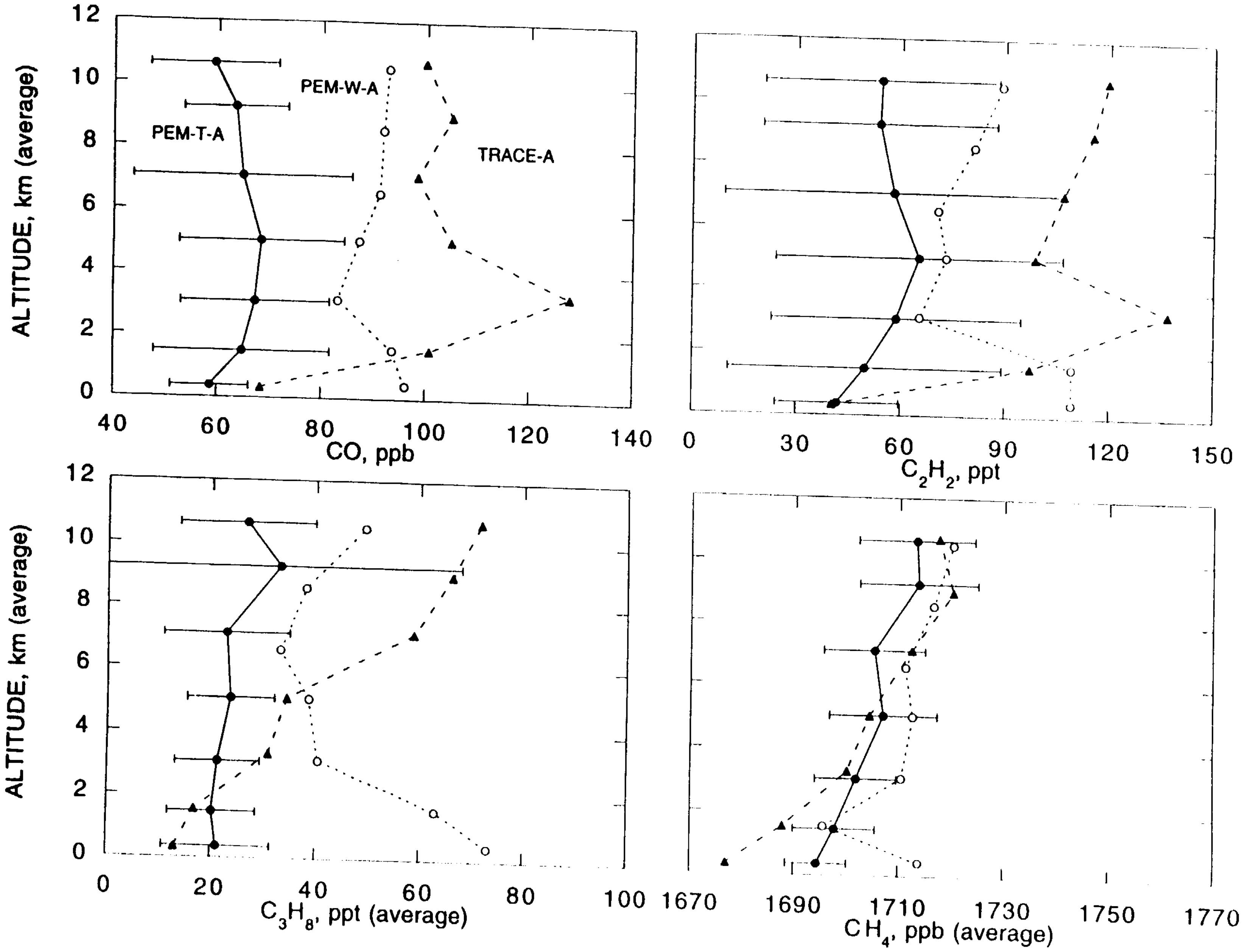
ALTITUDE, km (average)
12
10
8
6
4
2
0
PEM-T-A
PEM-W-A
TRACE-A
40
60
80
100
120
140
CO, ppb
0
30
60
90
120
150
C_2H_2, ppt
ALTITUDE, km (average)
0
20
40
60
80
100
C_3H_8, ppt (average)
1670
1690
1710
1730
1750
1770
CH_4, ppb (average)

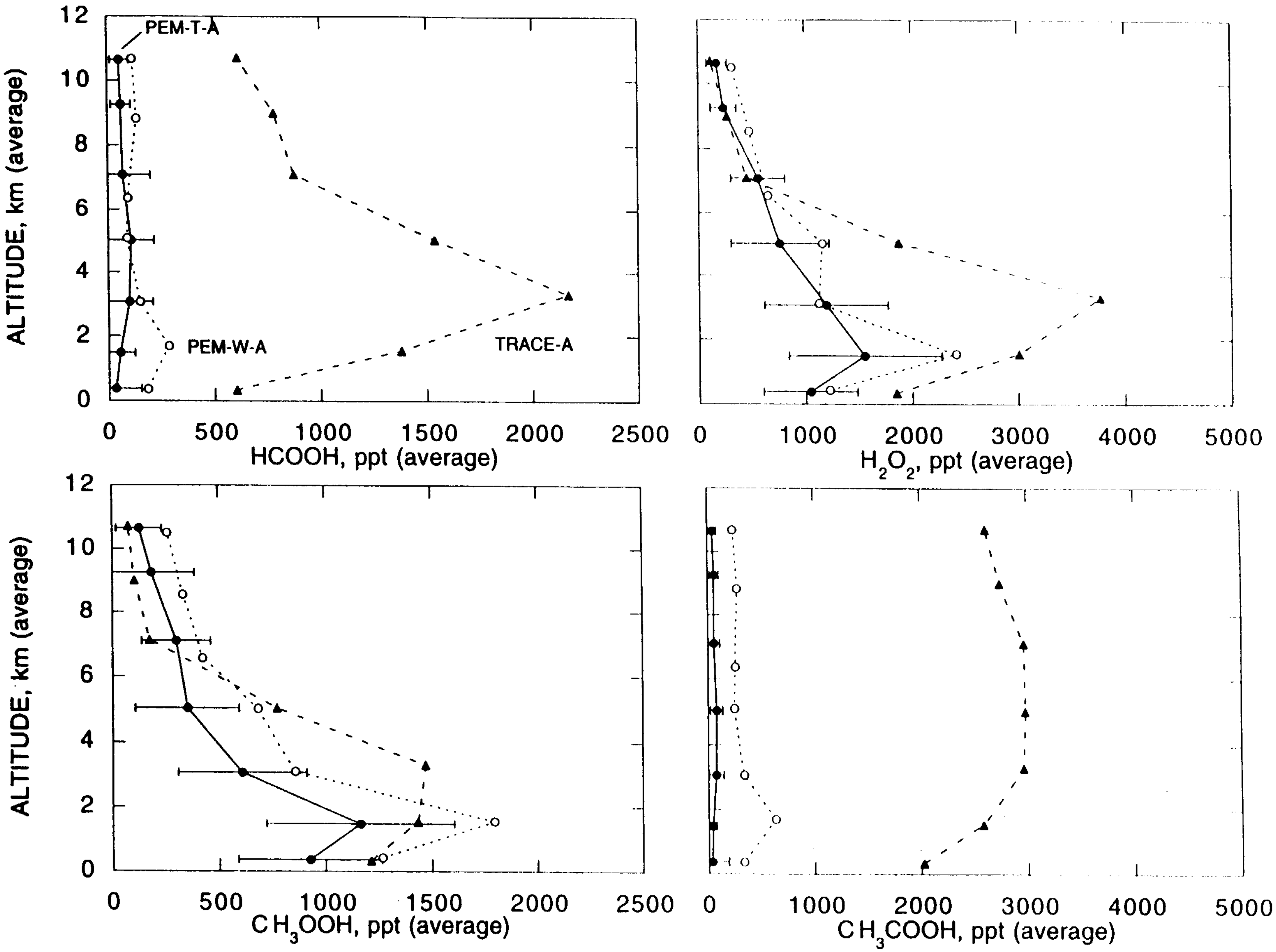
PEM-T-A
PEM-W-A
TRACE-A
ALTITUDE, km (average)
0
2
4
6
8
10
12
0
500
1000
1500
2000
2500
HCOOH, ppt (average)
0
1000
2000
3000
4000
5000
H_2O_2, ppt (average)
ALTITUDE, km (average)
CH_3OOH, ppt (average)
CH_3COOH, ppt (average)

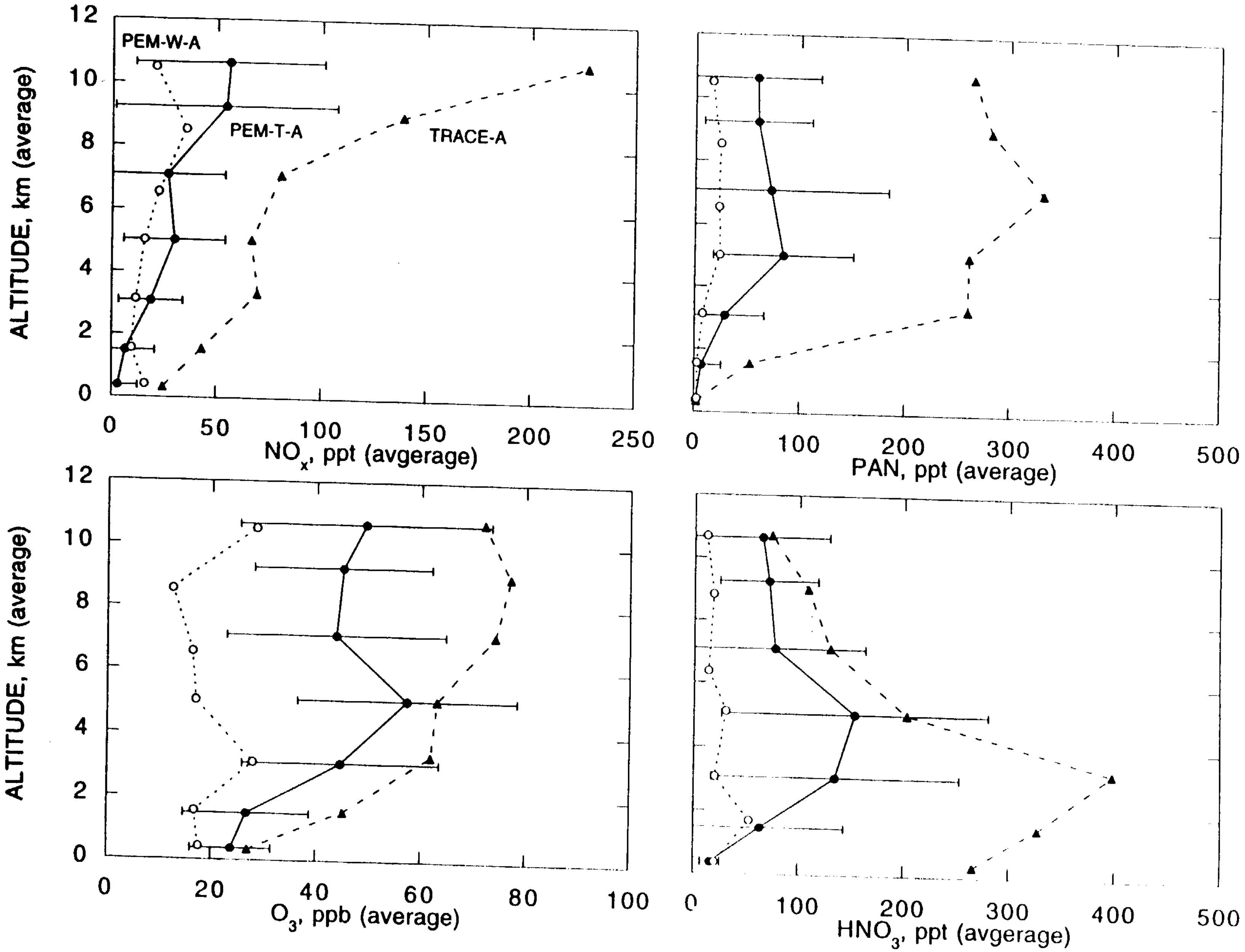
PEM-W-A
PEM-T-A
TRACE-A
ALTITUDE, km (average)
0
2
4
6
8
10
12
0
50
100
150
200
250
NO$_x$, ppt (avgerage)
0
100
200
300
400
500
PAN, ppt (average)
ALTITUDE, km (average)
0
20
40
60
80
100
O$_3$, ppb (average)
0
100
200
300
400
500
HNO$_3$, ppt (avgerage)

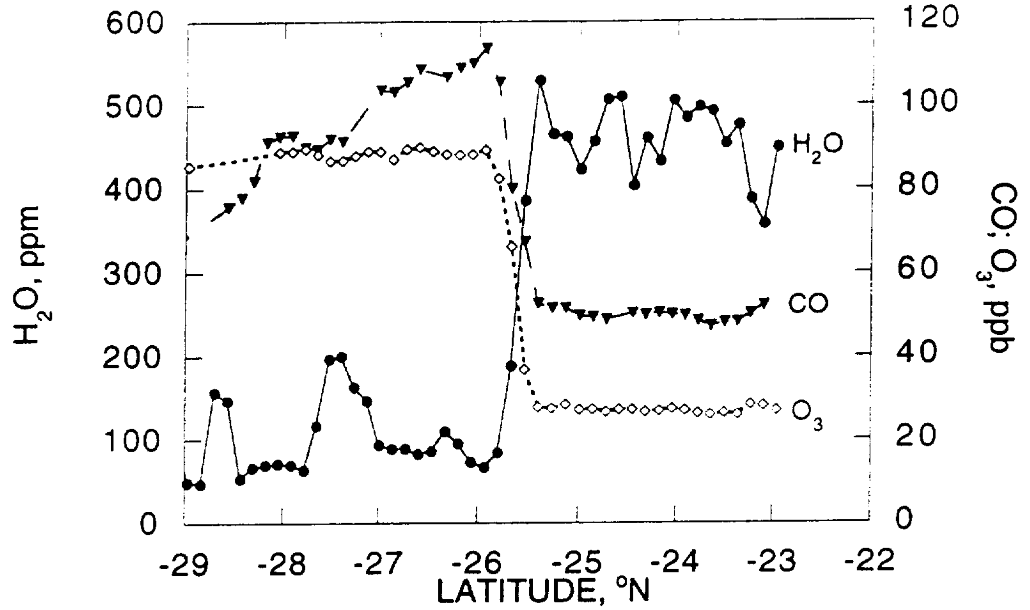
H$_2$O, ppm
CO; O$_3$, ppb
LATITUDE, °N
H$_2$O
CO
O$_3$
0
100
200
300
400
500
600
0
20
40
60
80
100
120
-29
-28
-27
-26
-25
-24
-23
-22

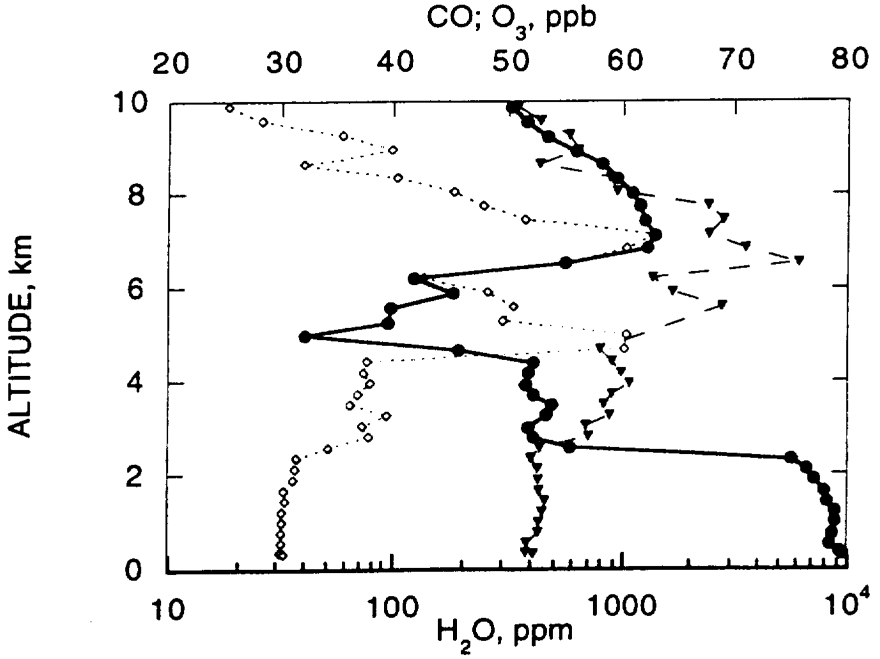
CO; O$_3$, ppb
20
30
40
50
60
70
80
ALTITUDE, km
0
2
4
6
8
10
H$_2$O, ppm
10
100
1000
10^4

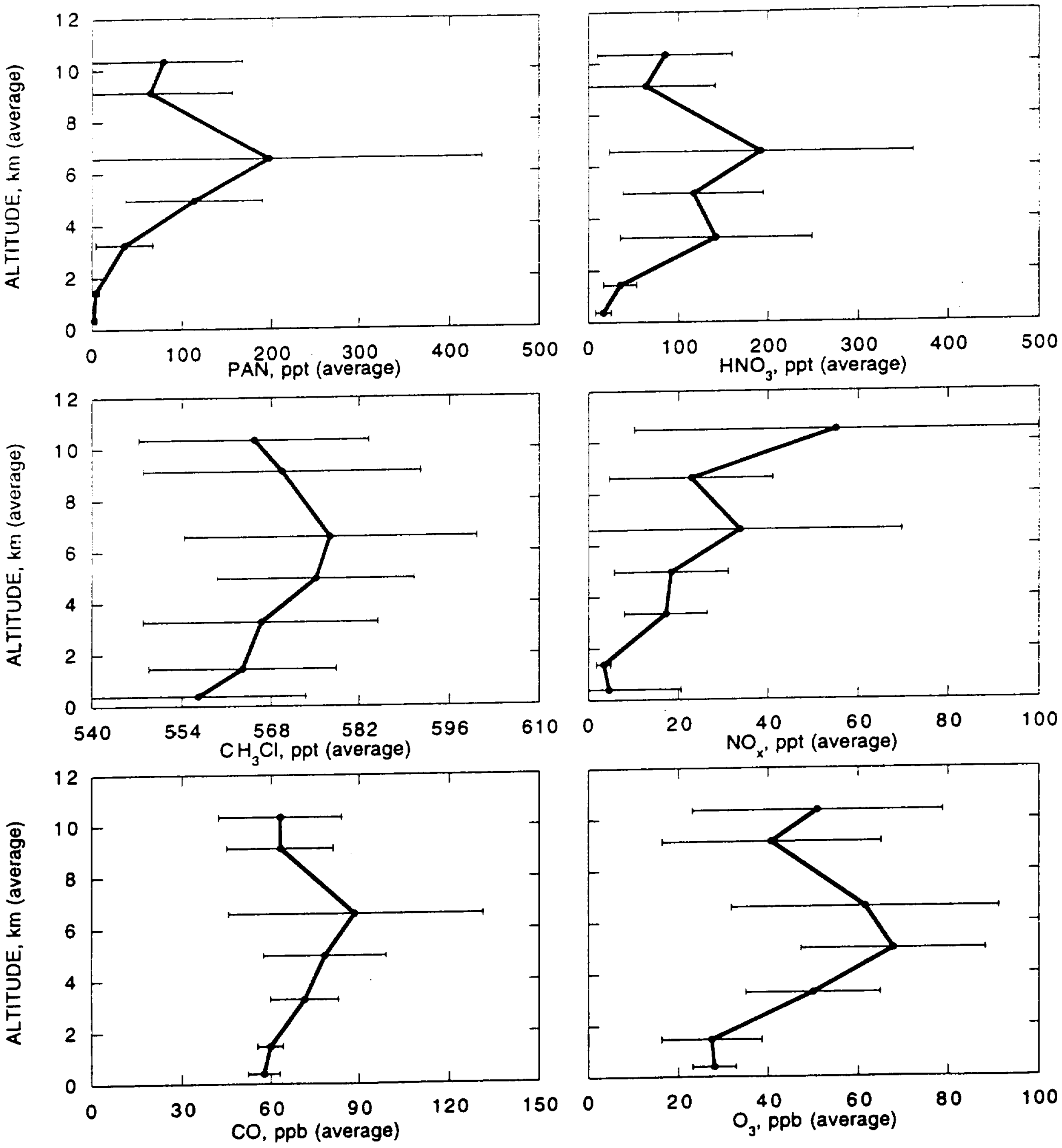
ALTITUDE, km (average)
0
2
4
6
8
10
12
0
100
200
300
400
500
PAN, ppt (average)
0
100
200
300
400
500
HNO$_3$, ppt (average)
540
554
568
582
596
610
CH$_3$Cl, ppt (average)
0
20
40
60
80
100
NO$_x$, ppt (average)
0
30
60
90
120
150
CO, ppb (average)
0
20
40
60
80
100
O$_3$, ppb (average)

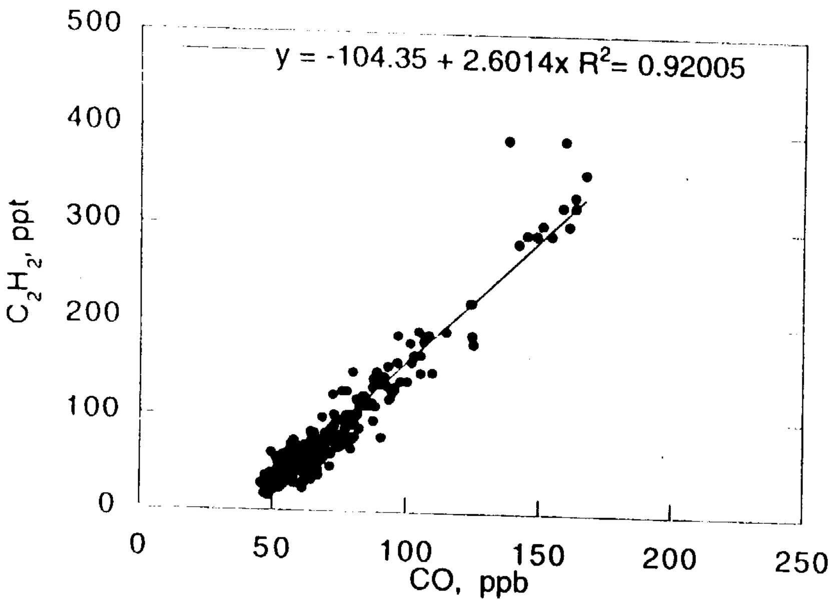
y = -104.35 + 2.6014x R^2= 0.92005
C_2H_2, ppt
0
100
200
300
400
500
0
50
100
150
200
250
CO, ppb

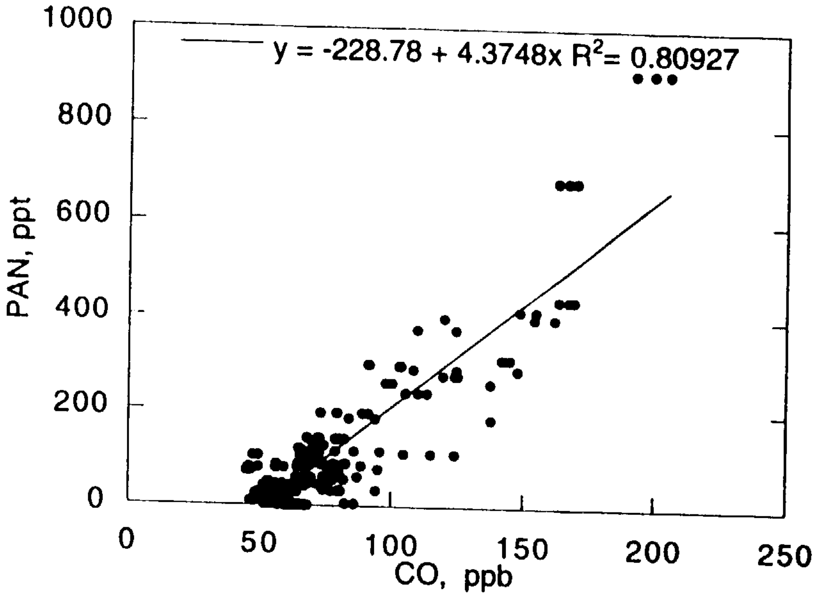
y = -228.78 + 4.3748x R^2= 0.80927
PAN, ppt
0
200
400
600
800
1000
0
50
100
150
200
250
CO, ppb